Intelligent Scatter Radio, RF Harvesting Analysis, and Resource Allocation for Ultra-Low-Power Internet-of-Things

Panos N. Alevizos
Thesis Supervisor: Aggelos Bletsas

September 29, 2017

Agenda

What is IoT? – Emerging Applications

- Global network infrastructure composed by a variety of devices interacting with each other through the Internet [1].
  - Fit to customer demands.
- IoT applications [1–3]:
  - Transportation and smart vehicles.
  - Smart buildings.
  - Industry.
  - Healthcare.
  - Environmental sensing.
- By 2020: 212 billion IoT devices.
- By 2025: 2.7–6.2 trillion $.

---

[1] L. Atzori, A. Iera, and G. Morabito, "The internet of things: A survey," *Computer networks*, 2010.
[2] L. Da Xu, W. He, and S. Li, "Internet of things in industries: A survey," *IEEE Trans. Ind. Informat.*, 2014.
[3] A. Al-Fuqaha *et al.* "Internet of things: A survey on enabling technologies, protocols, and applications," *IEEE Commun. Surveys Tuts.*, 2015.

Precision Agriculture

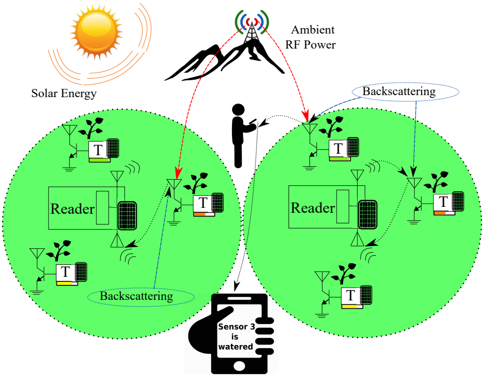

- 80-85% of total water is consumed for agriculture purposes.
- Intelligent plant irrigation:
  - Save 30% of water $\implies$ socioeconomic impact.

Dissertation Objectives

- Enhance ultra-low-power IoT technology exploiting novel concepts in wireless communications and networking.
- Objectives:
  - Accurate RF energy harvesting analysis.
  - Ultra-low complexity, increased range, small processing delay, scatter radio receivers.
  - New, flexible, scatter radio network architecture with extended coverage.
  - Resource allocation for multi-cell backscatter sensor networks (BSNs).

Problem Statement (1/2)

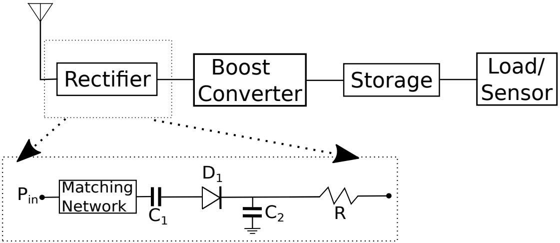

- Diodes in rectifier circuits:
  - Strong nonlinearities on power conversion.
  - Sensitivity and saturation effects.

Problem Statement (2/2)

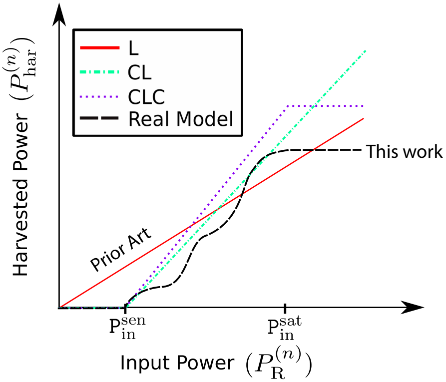

- Prior art in wireless communications uses linear model.
- This work offers accurate nonlinear RF harvesting analysis.

Wireless System Model

- Baseband narrowband received signal:

$$y = \sqrt{P_{\mathrm{T}}\, T_{\mathrm{s}}\, \mathsf{L}(d)}\, h\, s + w. \tag{1}$$

- Block fading model.
- Received power over n-th coherence block:

$$P_{\mathrm{R}}^{(n)} = \mathbb{E}\left[|s|^2\right] P_{\mathrm{T}}\, \mathsf{L}(d) \left|h^{(n)}\right|^2 = \mathsf{P}(d)\gamma^{(n)}. \tag{2}$$

- PDF of $\gamma^{(n)}$ continuous over $\mathbb{R}_+$, e.g., $\gamma^{(n)} \sim \mathrm{Gamma}\left(\mathtt{m}, \frac{\Omega}{\mathtt{m}}\right)$:

$$\mathsf{f}_{\gamma^{(n)}}(x) = \left(\frac{\mathtt{m}}{\Omega}\right)^{\mathtt{m}} \frac{x^{\mathtt{m}-1}}{\Gamma(\mathtt{m})}\, \mathsf{e}^{-\frac{\mathtt{m}}{\Omega}x}, \quad x \geq 0. \tag{3}$$

Harvesting Efficiency Models (1/2)

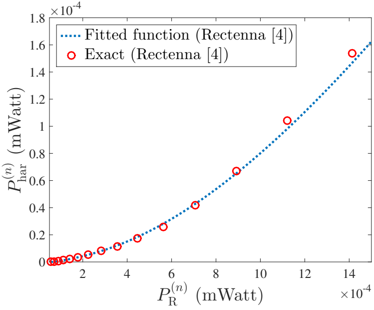

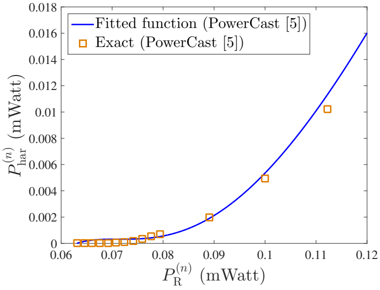

[4] S. D. Assimonis, S.-N. Daskalakis, and A. Bletsas, "Sensitive and efficient RF harvesting supply for batteryless backscatter sensor networks," *IEEE Trans. Microw. Theory Techn.*, 2016.
[5] PowerCast Module, http://www.mouser.com/ds/2/329/P2110B-Datasheet-Rev-3-1091766.pdf.

Harvesting Efficiency Models (2/2)

- Real model harvested power:

$$P_{\mathrm{har}}^{(n)} \equiv P_{\mathrm{har}}^{(n)}\left(P_{\mathrm{R}}^{(n)}\right) = \mathsf{p}\left(P_{\mathrm{R}}^{(n)}\right) \triangleq \begin{cases} 0, & P_{\mathrm{R}}^{(n)} \in [0, \mathrm{P}_{\mathrm{in}}^{\mathrm{sen}}], \\ \eta\left(P_{\mathrm{R}}^{(n)}\right) \cdot P_{\mathrm{R}}^{(n)}, & P_{\mathrm{R}}^{(n)} \in [\mathrm{P}_{\mathrm{in}}^{\mathrm{sen}}, \mathrm{P}_{\mathrm{in}}^{\mathrm{sat}}], \\ \eta(\mathrm{P}_{\mathrm{in}}^{\mathrm{sat}}) \cdot \mathrm{P}_{\mathrm{in}}^{\mathrm{sat}} & P_{\mathrm{R}}^{(n)} \in [\mathrm{P}_{\mathrm{in}}^{\mathrm{sat}}, \infty). \end{cases} \tag{4}$$

- Prior art:

$$\widetilde{\mathsf{p}}_{\mathrm{L}}\left(P_{\mathrm{R}}^{(n)}\right) = \eta_{\mathrm{L}} \cdot P_{\mathrm{R}}^{(n)}, \ \forall P_{\mathrm{R}}^{(n)} \in \mathbb{R}_{+}, \ \eta_{\mathrm{L}} \in [0, 1). \tag{5}$$

Proposed Approximation (1/2)

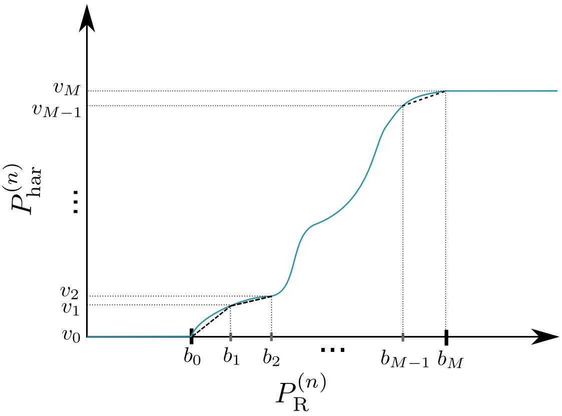

Proposed Approximation (2/2)

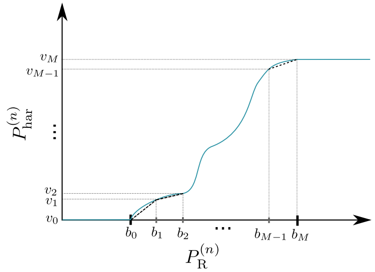

Theorem

The PDF of the proposed approximation model is

$$f_{\widetilde{P}_{\rm har}^{(n)}}(x) = \begin{cases} \xi_0\,\Delta(x), & x = v_0 = 0, \\ \frac{1}{l_m}\, f_{P_{\rm R}^{(n)}}\left(\frac{x - v_{m-1} + l_m b_{m-1}}{l_m}\right), & x \in (v_{m-1}, v_m] \setminus \{v_M\},\ m \in [M], \\ (1-\xi_M)\,\Delta(x - v_M), & x = v_M, \\ 0, & x \in \mathbb{R} \setminus [0, v_M], \end{cases} \tag{6}$$

with $\xi_m = F_{P_{\rm R}^{(n)}}(b_m)$, $m = 0, 1, \ldots, M$, $l_m \triangleq \frac{v_m - v_{m-1}}{b_m - b_{m-1}}$, $m = 1, 2, \ldots, M$.

Evaluation (1/2)

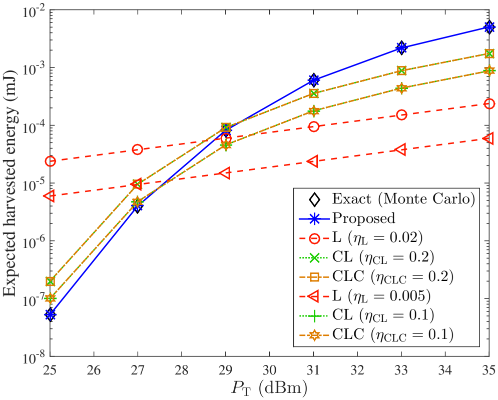

- Expected harvesting energy: $T_{\mathrm{p}}\,\mathbb{E}\left[\sum_{n=1}^{N} P_{\mathrm{har}}^{(n)}\right] = N\,T_{\mathrm{p}}\,\mathbb{E}\left[P_{\mathrm{har}}^{(n)}\right]$.

Evaluation (2/2)

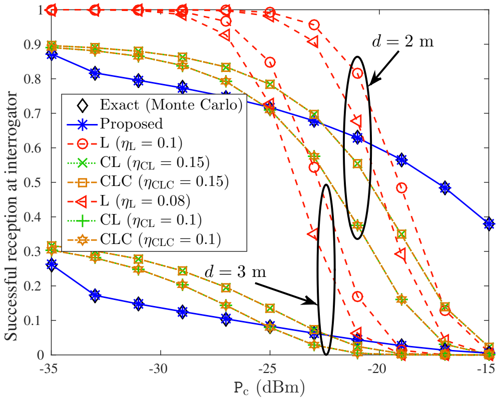

- Successful reception at interrogator: $\mathbb{P}(\mathcal{S}) \triangleq \mathbb{P}(\mathcal{A} \cap \mathcal{B})$.

Problem Statement (1/2)

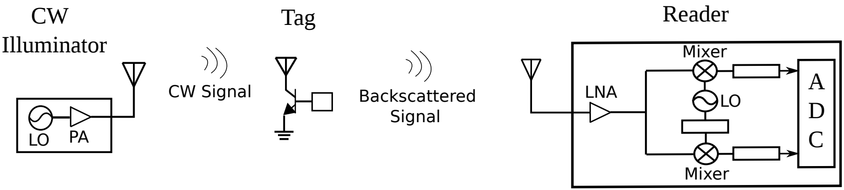

- Scatter Radios: Communication via means of reflection [6].
  - Ultra-low power
  - Low monetary cost.

[6] G. Vannucci, A. Bletsas, and D. Leigh, A software-defined radio system for backscatter sensor networks, *IEEE Trans. Wireless Commun.*, 2008.

Problem Statement (2/2)

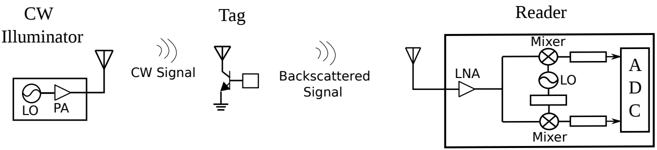

- Inherent problems:
  - Large path-loss attenuation $\Longrightarrow$ Limited range.
  - Passive tags $\Longrightarrow$ Powering issues $\Longrightarrow$ Limited range.
  - High bitrate $\Longrightarrow$ Reduced energy per bit $\Longrightarrow$ Limited range.
- This work:
  - Short-packet communication.
  - Optimal receiver design for scatter radio signals.

Wireless and Signal Model

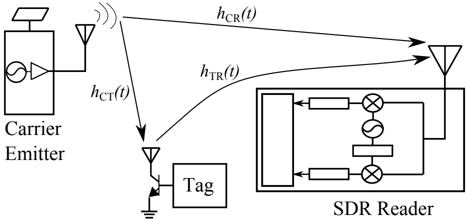

- Flat Rician fading: $h_{\mathrm{m}}(t) = h_{\mathrm{m}} \sim \mathcal{CN}\left(\sqrt{\frac{\kappa_{\mathrm{m}}}{\kappa_{\mathrm{m}}+1}}\sigma_{\mathrm{m}}, \frac{\sigma_{\mathrm{m}}^2}{\kappa_{\mathrm{m}}+1}\right)$, $\mathrm{m} \in \{\mathrm{CR}, \mathrm{CT}, \mathrm{TR}\}$ [7].
- Baseband signal for scatter radio FSK modulation [Theorem 1, 8]:

$$\mathbf{r} = [r_0^+ \; r_0^- \; r_1^+ \; r_1^-]^\top = h\sqrt{\frac{\mathrm{E}}{2}}[\mathrm{e}^{+\mathrm{j}\Phi_0} \; \mathrm{e}^{-\mathrm{j}\Phi_0} \; \mathrm{e}^{+\mathrm{j}\Phi_1} \; \mathrm{e}^{-\mathrm{j}\Phi_1}]^\top \odot \mathbf{s}_i + \mathbf{n}. \quad (7)$$

[7] A. Goldsmith, *Wireless Communications*, 2005.
[8] N. Fasarakis-Hilliard, P. N. Alevizos, and A. Bletsas, "Coherent detection and channel coding for bistatic scatter radio sensor networking," *IEEE Trans. Commun.*, 2015.

Noncoherent Symbol-by-Symbol Detectors (1/2)

- Statistics: $\mathrm{f}(\mathbf{r}|i,h,\mathbf{\Phi}) \equiv \mathcal{CN}\left(h\,\mathbf{x}_i(\mathbf{\Phi}), N_0\,\mathbf{I}_4\right)$, with $\mathbf{x}_i(\mathbf{\Phi}) = \sqrt{\frac{\mathrm{E}}{2}}\left[\mathrm{e}^{+\mathrm{j}\Phi_0}, \mathrm{e}^{-\mathrm{j}\Phi_0}, \mathrm{e}^{+\mathrm{j}\Phi_1}, \mathrm{e}^{-\mathrm{j}\Phi_1}\right]^\top \odot \mathbf{s}_i,\ \ i \in \mathbb{B}$.

Lemma

Noncoherent Hybrid Composite Hypothesis-Testing (NC-HCHT) Symbol-By-Symbol FSK Detection:

$$\arg\max_{i\in\mathbb{B}} \left\{ \mathbb{E}_{\mathbf{\Phi}} \left[\max_{h\in\mathbb{C}} \ln[\mathrm{f}(\mathbf{r}|i,h,\mathbf{\Phi})] \right] \right\} \Longleftrightarrow |r_0^+|^2 + |r_0^-|^2 \underset{i=1}{\overset{i=0}{\gtrless}} |r_1^+|^2 + |r_1^-|^2. \quad (8)$$

Noncoherent Symbol-by-Symbol Detectors (2/2)

- Statistics: $\mathrm{f}(\mathbf{r}|i,h,\boldsymbol{\Phi}) \equiv \mathcal{CN}\left(h\,\mathbf{x}_i(\boldsymbol{\Phi}), N_0\,\mathbf{I}_4\right)$, with $\mathbf{x}_i(\boldsymbol{\Phi}) = \sqrt{\frac{\mathrm{E}}{2}}\left[\mathrm{e}^{+\mathrm{j}\Phi_0}, \mathrm{e}^{-\mathrm{j}\Phi_0}, \mathrm{e}^{+\mathrm{j}\Phi_1}, \mathrm{e}^{-\mathrm{j}\Phi_1}\right]^\top \odot \mathbf{s}_i,\ \ i \in \mathbb{B}$.

Theorem

Noncoherent Generalized Likelihood-Ratio Test (NC-GLRT) Symbol-By-Symbol FSK Detection:

$$\arg\max_{i\in\mathbb{B}}\left\{\max_{\boldsymbol{\Phi}\in[0,2\pi)^2}\max_{h\in\mathbb{C}}\ln[\mathrm{f}(\mathbf{r}|i,h,\boldsymbol{\Phi})]\right\} \Longleftrightarrow |r_0^+| + |r_0^-| \underset{i=1}{\overset{i=0}{\gtrless}} |r_1^+| + |r_1^-|. \quad (9)$$

Noncoherent GLRT Sequence Detector

- Static environments: Coherence time $\geq$ Packet duration.
- Transmitted sequence: $\mathbf{i} = [i_1 \; i_2 \; \dots \; i_{N_\mathrm{s}}]^\top \in \mathbb{B}^{N_\mathrm{s}}$.
- Received sequence: $\mathbf{r}_{1:N_\mathrm{s}}$ with statistics

$$\mathrm{f}(\mathbf{r}_{1:N_\mathrm{s}} | \mathbf{i}, h, \mathbf{\Phi}) \equiv \mathcal{CN}\left(h \, \mathbf{x}_\mathbf{i}(\mathbf{\Phi}), N_0 \, \mathbf{I}_{4N_\mathrm{s}}\right). \quad (10)$$

- GLRT sequence detector:

$$\mathbf{i}_{\mathrm{GLRT}} = \arg \max_{\mathbf{i} \in \mathbb{B}^{N_\mathrm{s}}} \max_{\mathbf{\Phi} \in [0, 2\pi)^2} \max_{h \in \mathbb{C}} \ln[\mathrm{f}(\mathbf{r}_{1:N_\mathrm{s}} | \mathbf{i}, h, \mathbf{\Phi})]. \quad (11)$$

Theorem

There exists algorithm that finds $\mathbf{i}_{\mathrm{GLRT}}$ with complexity $\mathcal{O}(N_\mathrm{s} \log N_\mathrm{s})$, based on [9].

[9] P. N. Alevizos, Y. Fountzoulas, G. N. Karystinos, and A. Bletsas, "Log-linear complexity GLRT-optimal noncoherent sequence detection for orthogonal and RFID-oriented modulations," *IEEE Trans. Commun.*, 2016.

Noncoherent HCHT Soft-decision Decoding

- Diminsish long-bursts of fading: interleaving of depth D.
- Baseband coded signal using interleaving:

$$\mathbf{r}_{1:N_c} = \begin{bmatrix} \mathbf{r}_1 \\ \mathbf{r}_2 \\ \vdots \\ \mathbf{r}_{N_c} \end{bmatrix} = \begin{bmatrix} h_1 \mathbf{x}_{c_1}(\mathbf{\Phi}) \\ h_2 \mathbf{x}_{c_2}(\mathbf{\Phi}) \\ \vdots \\ h_{N_c} \mathbf{x}_{c_{N_c}}(\mathbf{\Phi}) \end{bmatrix} + \begin{bmatrix} \mathbf{n}_1 \\ \mathbf{n}_2 \\ \vdots \\ \mathbf{n}_{N_c} \end{bmatrix}. \tag{12}$$

Theorem

For $DT \geq T_{\text{coh}}$, noncoherent HCHT soft-decision decoding

$$\arg\max_{\mathbf{c}\in\mathcal{C}} \left\{ \mathbb{E}_{\mathbf{\Phi}} \left[\max_{\mathbf{h}\in\mathbb{C}^{N_c}} \ln[f(\mathbf{r}_{1:N_c}|\mathbf{c},\mathbf{h},\mathbf{\Phi})] \right] \right\} \Longleftrightarrow \arg\max_{\mathbf{c}\in\mathcal{C}} \sum_{n=1}^{N_c} w_n c_n, \tag{13}$$

where $w_n \triangleq |r_1^+(n)|^2 + |r_1^-(n)|^2 - \left(|r_0^+(n)|^2 + |r_0^-(n)|^2\right)$, $n = 1, 2, \ldots, N_c$.

Numerical Results (1/2)

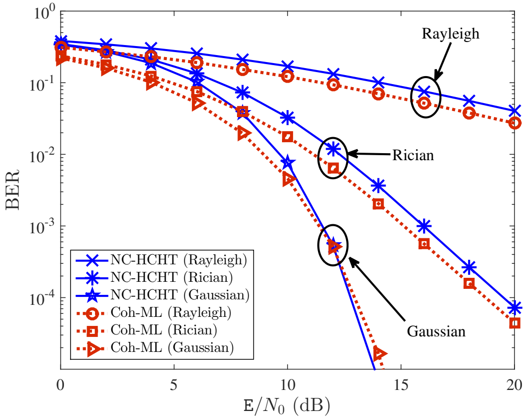

- Wireless and signal parameters: $T = 1$ msec, $T_{\text{coh}} = 100$ msec, 30 training bits.

Numerical Results (2/2)

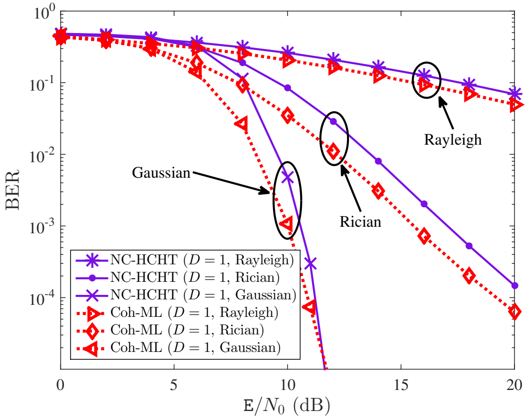

- Wireless and signal parameters: $T = 1$ msec, $T_{\text{coh}} = 100$ msec, 30 training bits.

Experimental Results (1/2)

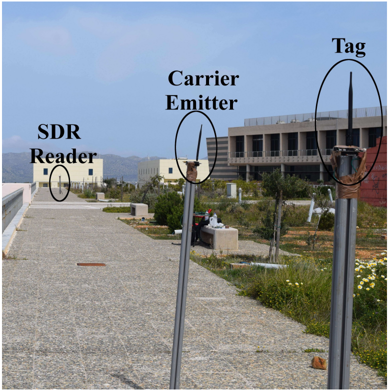

- Parameters: $d_{\mathrm{CT}} = 8$ m, $T = 1$ msec, $F_1 = 2F_0 = 250$ kHz, 16 training + 31 data coded bits.

Experimental Results (2/2)

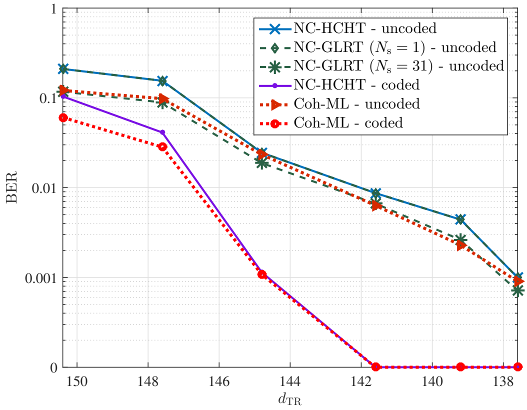

- Reception algorithms: Energy-based synchronization, Periodogram-based CFO estimation.

Problem Statement (1/2)

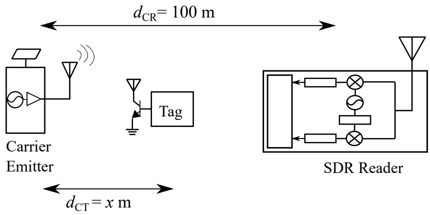

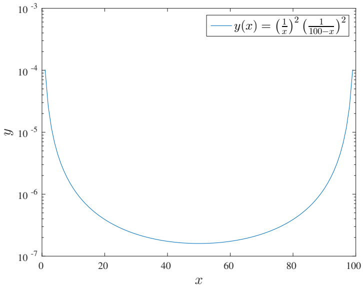

- Asymmetric scatter radio architecture can reduce path-loss:
  - $\mathrm{PL} \propto y(x) = \left(\frac{1}{x}\right)^2 \left(\frac{1}{100-x}\right)^2$.
  - $y(x)$ is minimized at $x = d/2 = 50$ m.
  - $y(x)$ increases as $x \longrightarrow 0$ or $x \longrightarrow 100$.

Problem Statement (2/2)

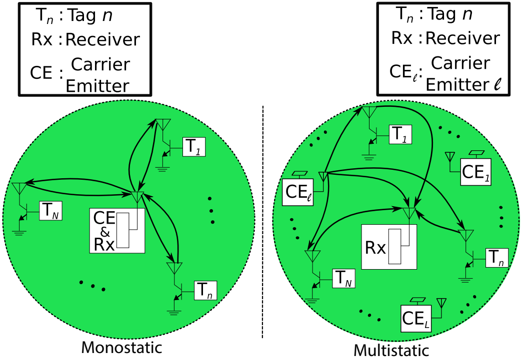

- This work proposes multistatic architecture.
- Outperforms globally state-of-the-art monostatic architecture.

BER Analysis (1/2)

Theorem

Under dyadic Nakagami fading, the BER of monostatic architecture with ML coherent detection can be bounded as

$$\mathbb{P}\left(e_{l,n}^{[\mathrm{m}]}\right) \leq \frac{1}{2}\left(\frac{\mathtt{M}_n + \mathtt{M}_n^2}{2\,\mathtt{SNR}_n^{[\mathrm{m}]}}\right)^{\frac{\mathtt{M}_n}{2}} \mathsf{U}\left(\frac{\mathtt{M}_n}{2}, \frac{1}{2}, \frac{\mathtt{M}_n + \mathtt{M}_n^2}{2\,\mathtt{SNR}_n^{[\mathrm{m}]}}\right), \tag{14}$$

where $\mathtt{M}_n$ is the Nakagami parameter for link TR, and $\mathsf{U}(\cdot,\cdot,\cdot)$ is given in [Eq. (13.4.4), 10], and $\mathtt{SNR}_n^{[\mathrm{m}]}$ is the average received SNR for monostatic system. For dyadic Rayleigh fading ($\mathtt{M}_n = 1$), the corresponding diversity order is $-\frac{1}{2}$.

- The above BER expression coincides with noncoherent envelope monostatic scatter radio detection.

[10] F. W. J. Olver *et. al*, *NIST handbook of mathematical functions*, 2010.

BER Analysis (2/2)

Theorem

Under dyadic Nakagami fading, the BER of bistatic architecture with ML coherent detection can be bounded as

$$\mathbb{P}\left(e_{l,n}^{[\mathrm{b}]}\right) \leq \frac{1}{2}\left(\frac{2\,\mathtt{M}_{ln}\mathtt{M}_{n}}{\mathtt{SNR}_{l,n}^{[\mathrm{b}]}}\right)^{\mathtt{M}_{n}} \mathsf{U}\left(\mathtt{M}_{n}, 1+\mathtt{M}_{n}-\mathtt{M}_{ln}, \frac{2\,\mathtt{M}_{ln}\mathtt{M}_{n}}{\mathtt{SNR}_{l,n}^{[\mathrm{b}]}}\right), \qquad (15)$$

where $\mathtt{M}_{n}$ and $\mathtt{M}_{ln}$ are the Nakagami parameters for links TR and CT, respectively, while $\mathtt{SNR}_{l,n}^{[\mathrm{b}]}$ is the average received SNR for bistatic system. Under dyadic Rayleigh fading ($\mathtt{M}_{n} = \mathtt{M}_{ln} = 1$), the diversity order is -1.

- The above BER expression coincides with noncoherent envelope bistatic scatter radio detection.

Numerical Results (1/2)

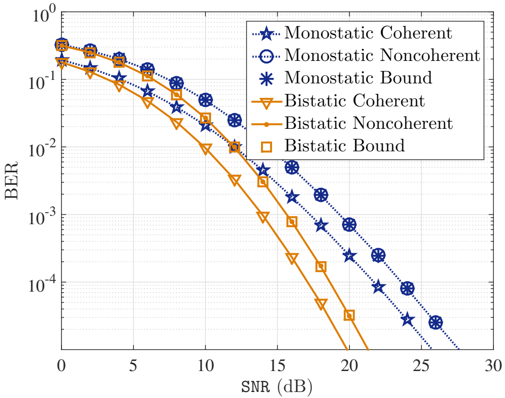

- Wireless and signal parameters: Equal average received SNR, $\mathtt{M}_n = 5.7619$ and $\mathtt{M}_{ln} = 5.2632$.

Numerical Results (2/2)

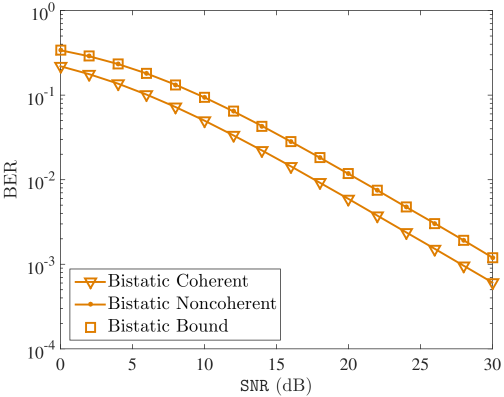

- Wireless and signal parameters: $\mathtt{M}_n = 5.7619$ and $\mathtt{M}_{ln} = 1$.

Problem Statement

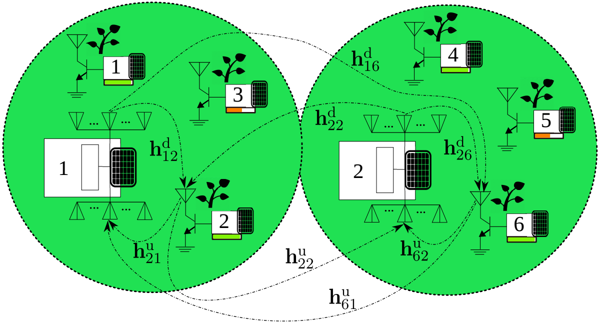

- Resource allocation in multi-cell BSNs:
  - Maximize coverage.
  - Reduce installation cost.

System Model

- Cores, tags, and frequency sub-channels: $\mathcal{B}$, $\mathcal{K}$, $\mathcal{C}$.
- Rician MIMO wireless downlink and uplink channels between core b and tag k: $\mathbf{h}_{bk}^{\mathrm{d}}$ and $\mathbf{h}_{kb}^{\mathrm{u}}$.
- Orthogonal pilot sequences $\left\{\mathbf{x}^{(1)}, \mathbf{x}^{(2)}, \ldots, \mathbf{x}^{(M_{\mathrm{tr}})}\right\} \subset \{\pm 1\}^{M_{\mathrm{tr}}}$.
- C orthogonal frequency sub-channels.
- Sets: $\mathcal{K}_{\mathcal{C}}(c)$, $\mathcal{K}_{\mathcal{B}}(b)$, $\mathcal{K}_{\mathcal{M}_{\mathrm{tr}}}(m)$, $\mathcal{K}_{bmc} = \mathcal{K}_{\mathcal{B}}(b) \cap \mathcal{K}_{\mathcal{M}_{\mathrm{tr}}}(m) \cap \mathcal{K}_{\mathcal{C}}(c)$.

Theorem

The baseband signal at core $b \in \mathcal{B}$ over the i-th time instant, at the output of c-th frequency filter is

$$\mathbf{r}_{b,i}^{(c)} = \sum_{k \in \mathcal{K}_{\mathcal{C}}(c)} \boldsymbol{\xi}_{kb}^{(c)} x_{k,i} + \mathbf{n}_{b,i}^{(c)}, \quad i = 1, 2, \ldots, M. \tag{16}$$

Mult-Cell Training Signal

- Training signal for tag $k \in \mathcal{K}_{bmc}$, $|\mathcal{K}_{bmc}| = 1$:

$$\widetilde{\mathbf{R}}_{b,\mathrm{tr}}^{(c)} \frac{\mathbf{x}^{(m)}}{\left\|\mathbf{x}^{(m)}\right\|_2^2} \triangleq \mathbf{r}_{b,\mathrm{tr}}^{(c)} = \boldsymbol{\xi}_{kb}^{(c)} + \sum_{b' \neq b} \sum_{k' \in \mathcal{K}_{b' mc}} \boldsymbol{\xi}_{k'b}^{(c)} + \mathbf{v}_{b,\mathrm{tr}}^{(c)}, \qquad (17)$$

Proposition

For vectors $\{\boldsymbol{\xi}_{kb}^{(c)}\}_{k \in \mathcal{K}_{\mathcal{C}}(c)}, \forall c \in \mathcal{C}, \forall b \in \mathcal{B}$, mean $\mathbb{E}[\boldsymbol{\xi}_{kb}^{(c)}] = \mathbf{0}_{N_{\mathrm{R}}}$ and covariance $\mathbf{C}_{\boldsymbol{\xi}_{kb}^{(c)}}$ can be found in closed-form.

Multi-Cell CSI Acquisition and Linear Detection

Theorem

For a tag $k \in \mathcal{K}_{bmc}$ the LMMSE estimate of $\boldsymbol{\xi}_{kb}^{(c)}$ based on training signal $\mathbf{r}_{b,\mathrm{tr}}^{(c)}$ is given by

$$\widehat{\boldsymbol{\xi}}_{kb}^{(c)} = \mathbf{C}_{\boldsymbol{\xi}_{kb}^{(c)}} \left(\sum_{b' \in \mathcal{B}} \sum_{k' \in \mathcal{K}_{b'mc}} \mathbf{C}_{\boldsymbol{\xi}_{k'b}^{(c)}} + \frac{N_0}{M_{\mathrm{tr}}^2} \mathbf{I}_{N_{\mathrm{R}}} \right)^{-1} \mathbf{r}_{b,\mathrm{tr}}^{(c)}. \tag{18}$$

Vectors $\widehat{\boldsymbol{\xi}}_{kb}^{(c)}$ and error vector $\boldsymbol{\epsilon}_{kb}^{(c)} = \widehat{\boldsymbol{\xi}}_{kb}^{(c)} - \boldsymbol{\xi}_{kb}^{(c)}$ are uncorrelated.

- Linear detection $\mathrm{sign}(\Re\{z_{k,i}\})$ for tag $k \in \mathcal{K}_{bmc}$, $z_{k,i} = (\mathbf{a}_{kb}^{(c)})^{\mathrm{H}}\, \mathbf{r}_{b,i}^{(c)}$.
  - Maximum-ratio combining (MRC).
  - Zero-forcing (ZF).

SINR Calculation and Problem Formulation

- Measure long-term SINR for pair $(k, c) \in \mathcal{K} \times \mathcal{C}$: $\overline{\texttt{SINR}}_{kb}^{(c)}$.
- Assign frequency sub-channels to tags $k \in \mathcal{K}_{\mathcal{B}}(b)$ according to:

$$\begin{aligned}
\text{maximize} \quad & \sum_{k \in \mathcal{K}_{\mathcal{B}}(b)} \sum_{c \in \mathcal{C}} \mathrm{g}\left(\overline{\texttt{SINR}}_{kb}^{(c)}\right) \cdot v_{kc} && \text{(19a)} \\
\text{subject to} \quad & \sum_{k \in \mathcal{K}_{bm}} v_{kc} \leq 1, \ \forall (m, c) \in \mathcal{M}_{\mathrm{tr}} \times \mathcal{C}, && \text{(19b)} \\
& \sum_{c \in \mathcal{C}} v_{kc} = 1, \ \forall k \in \mathcal{K}_{\mathcal{B}}(b), && \text{(19c)} \\
& v_{kc} \in \mathbb{B}, \ \forall (k, c) \in \mathcal{K}_{\mathcal{B}}(b) \times \mathcal{C}. && \text{(19d)}
\end{aligned}$$

Resource Allocation Algorithm (1/2)

Theorem

The FG message-passing update rules to solve optimally resource allocation problem (19)

$$\phi_{kc}^{(n)} = \max_{c' \in \mathcal{C} \setminus c} \left\{ -\rho_{kc'}^{(n-1)} + \mathrm{g}\left(\overline{\mathtt{SINR}}_{kb}^{(c')} \right) \right\}, \tag{20}$$

$$\rho_{kc}^{(n)} = \left[\max_{k' \in \mathcal{K}_{bm} \setminus k} \left\{ -\phi_{k'c}^{(n)} + \mathrm{g}\left(\overline{\mathtt{SINR}}_{k'b}^{(c)} \right) \right\} \right]^{+}, \quad k \in \mathcal{K}_{bm}, \tag{21}$$

where $[x]^{+} \triangleq \max\{x, 0\}$. Moreover, to infer the value for variable $v_{kc} \in \mathbb{B}$ at the n-th iteration,

$$\widehat{v}_{kc}^{(n)} = 1\left\{ \phi_{kc}^{(n)} + \rho_{kc}^{(n)} \leq \mathrm{g}\left(\overline{\mathtt{SINR}}_{kb}^{(c)} \right) \right\}. \tag{22}$$

Resource Allocation Algorithm

- Amenable to distributed implementation.
- If LP has integral and unique solution then message passing converges to the exact solution after $\mathcal{O}(C\,|\mathcal{K}_{\mathcal{B}}(b)|)$ iterations [11].
- Per iteration computation cost: $\mathcal{O}(C\,|\mathcal{K}_{\mathcal{B}}(b)|^2 + C^2|\mathcal{K}_{\mathcal{B}}(b)|)$.
- 5 to 15 iterations suffice for the algorithm to converge.

[11] M. Bayati, C. Borgs, J. Chayes, and R. Zecchina, "Belief propagation for weighted *b*-matchings on arbitrary graphs and its relation to linear programs with integer solutions," *SIAM Journal on Discrete Mathematics*, 2011.

Numerical Results (1/3)

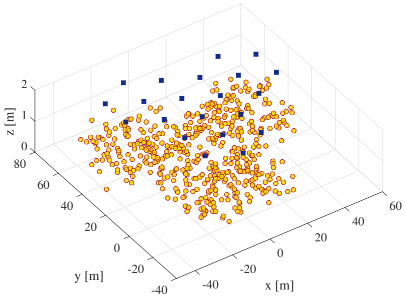

- Wireless and signal parameters: $B = 21$, $K = 500$, $C = 15$, $M_{\mathrm{tr}} = 8$, $\kappa^{\mathrm{u}}_{kb} = \kappa^{\mathrm{d}}_{bk} = 10$ dB, $\sigma^2_{bk} = \sigma^2_{kb} = \left(\frac{d_0}{\mathrm{d}_{bk}}\right)^{\nu_{bk}} \left(\frac{\lambda}{4\pi d_0}\right)^2$, with $\nu_{bk} = 2.1$, $\Gamma_{k,0} = 0.92$ and $\Gamma_{k,1} = -0.91$, $\eta_k = 0.2$, $\mathtt{f}^{(c)} = \frac{2c}{T}$, with $T = 0.1$ msec, $\sigma^2_b = -170$ dBm/Hz.

Numerical Results (2/3)

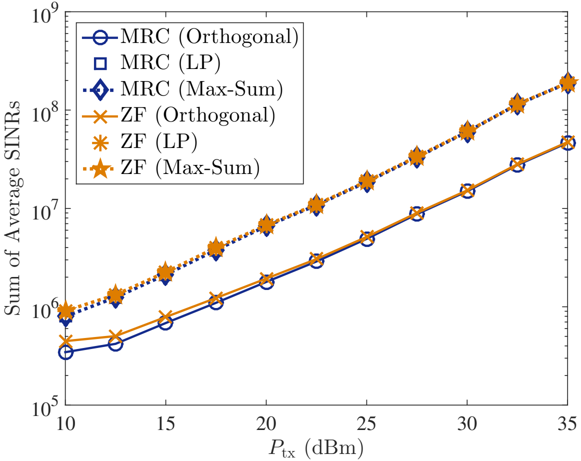

Numerical Results (3/3)

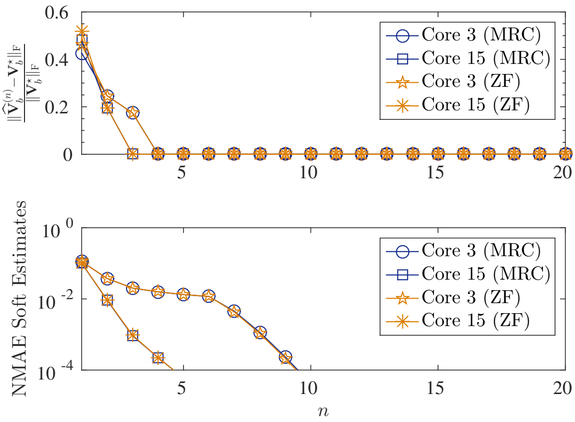

Contributions

- Enhance ultra-low-power IoT technology exploiting novel concepts in wireless communications and networking.
- Objectives:
  - Accurate RF energy harvesting analysis.
  - Ultra-low complexity, increased range, small processing delay, scatter radio receivers.
  - New, flexible, scatter radio network architecture with extended coverage.
  - Resource allocation for multi-cell backscatter sensor networks (BSNs).

Future Work

- Accurate resource allocation with nonlinear RF energy harvesting.
- Multistatic scatter radio cooperative localization.
- Linear detection performance analysis in multi-cell BSNs and comparison with existing WSN technology.

Acks

- Special thanks to Prof. A. Bletsas and the group:
    - G. Vougioukas, P. Oikonomakos, N. Psaromanolakis, J. Tsetis, M. Vestakis, L. Tsagkarakis, E. Stratigi, G. Sdoukopoulou, N. Ntantidakis, E. Giannelos, M. Ouroutzoglou.

Questions?

- Thank You!!

Conference Publications

10 **P. N. Alevizos** and A. Bletsas, "Scatter Radio Receivers for Extended Range Environmental Sensing WSNs, in Proc. IEEE Communication Theory Workshop (CTW), May 2016, Nafplio, Greece. *Student and Early Researcher Travel Grant Award*.

9 K. Tountas, **P. N. Alevizos**, A. Tzedaki, and A. Bletsas, "Bistatic Architecture Provides Extended Coverage and System Reliability in Scatter Sensor Networks", in Proc. International Eurasip Workshop on RFID Technology, Rosenheim, Germany, Oct. 2015.

8 N. Fasarakis-Hilliard, **P. N. Alevizos**, and A. Bletsas, "Coherent Detection and Channel Coding for Bistatic Scatter Radio Sensor Networking", in Proc. IEEE ICC, London, UK, Jun. 2015.

7 **P. N. Alevizos** and A. Bletsas, "Noncoherent Composite Hypothesis Testing Receivers for Extended Range Bistatic Scatter Radio WSNs," in Proc. IEEE ICC, London, UK, Jun. 2015.

6 **P. N. Alevizos**, Y. Foutzoulas, G. N. Karystinos, and A. Bletsas, "Noncoherent Sequence Detection of Orthogonally Modulated Signals in Flat Fading with Log-Linear Complexity," in Proc. IEEE ICASSP, Brisbane, Australia, Apr. 2015, *Conference-wide Student Paper Award and Best Student Paper Award in Communications and Networks track*.

5 N. Fasarakis-Hilliard, **P. N. Alevizos**, and A. Bletsas, "Variational Inference Cooperative Network Localization with Narrowband Radios," in Proc. IEEE ICASSP, Brisbane, Australia, Apr. 2015.

4 **P. N. Alevizos**, E. Vlachos, and A. Bletsas, "Factor Graph-based Distributed Frequency Allocation in Wireless Sensor Networks," in Proc. IEEE GLOBECOM, Austin, TX, USA, Dec. 2014.

3 N. Fasarakis-Hilliard, **P. N. Alevizos**, and A. Bletsas, "Narrowband Cooperative Network Localization," in Proc. IEEE GLOBECOM, Austin, TX, USA, Dec. 2014.

2 **P. N. Alevizos**, N. Fasarakis-Hilliard, K. Tountas, N. Agadakos, N. Kargas, and A. Bletsas, "Channel Coding for Increased Range Bistatic Backscatter Radio: Experimental Results," in Proc. IEEE RFID-TA, Tampere, Finland, Sep. 2014.

1 **P. N. Alevizos**, N. Fasarakis-Hilliard, and A. Bletsas, "Cooperative Localization in Wireless Sensor Networks under Bandwidth Constrains," in Proc. ASILOMAR, Pacific Grove, CA, USA, Nov. 2012.

Journal Publications

7 **P. N. Alevizos** and A. Bletsas, "Non-Linear Far Field RF Harvesting in Wireless Communications," submitted to IEEE Transactions on Wireless Communications (TWC), Jul. 2017, currently at second review round.

6 **P. N. Alevizos**, K. Tountas, and A. Bletsas, "Multistatic Scatter Radio Sensor Networks for Extended Coverage," submitted to IEEE Transactions on Wireless Communication (TWC), May 2017, currently at second review round.

5 **P. N. Alevizos**, E. Vlachos and A. Bletsas, "Inference-based Distributed Channel Allocation in Wireless Sensor Networks," Arxive.org.

4 **P. N. Alevizos**, A. Bletsas, G. N. Karystinos, "Noncoherent Short Packet Detection and Decoding for Scatter Radio Sensor Networking," IEEE Transactions on Communications (TCOM), Vol. 65, No. 5, pp. 2128-2140, May 2017.

3 **P. N. Alevizos** and A. Bletsas, "Network Localization Cramér-Rao Bounds for General Measurement Models," IEEE Communications Letters, Vol. 20, No. 9, pp. 1840-1843, Sept. 2016.

2 **P. N. Alevizos**, Y. Fountzoulas, G. N. Karystinos, and A. Bletsas, "Log-linear-complexity GLRT-optimal Noncoherent Sequence Detection for Orthogonal and RFID-oriented Modulations," IEEE Transactions on Communications (TCOM), Vol. 64, No. 4, pp. 1600-1612, Apr. 2016.

1 N. Fasarakis-Hilliard, **P. N. Alevizos**, and A. Bletsas, "Coherent Detection and Channel Coding for Bistatic Scatter Radio Sensor Networking," IEEE Transactions on Communications (TCOM), Vol. 63, No. 5, pp. 1798-1810, May 2015.